



Reactive oxygen species trigger NF- κ B-mediated NLRP3 inflammasome activation involvement in low-dose CdTe QDs exposure-induced hepatotoxicity

Yanting Pang, Daming Wu, Ying Ma, Yuna Cao, Qing Liu, Meng Tang, Yuepu Pu, Ting Zhang^{*}

Key Laboratory of Environmental Medicine Engineering, Ministry of Education, School of Public Health, Southeast University, Nanjing, 210009, China

ARTICLE INFO

Keywords:

Cd telluride quantum dots
Low-dose exposure
Reactive oxygen species
Hepatic macrophages (Kupffer cell)
NLRP3 inflammasome

ABSTRACT

Cadmium telluride (CdTe) quantum dots (QDs) can be employed as imaging and drug delivery tools; however, the toxic effects and mechanisms of low-dose exposure are unclear. Therefore, this pioneering study focused on hepatic macrophages (Kupffer cells, KCs) and explored the potential damage process induced by exposure to low-dose CdTe QDs. *In vivo* results showed that both 2.5 μ M/kg-bw and 10 μ M/kg-bw could both activate KCs to cause liver injury, and produce inflammation by disturbing antioxidant levels. Abnormal liver function further verified the risks of low-dose exposure to CdTe QDs. The KC model demonstrated that low-dose CdTe QDs (0 nM, 5 nM and 50 nM) can be absorbed by cells and cause severe reactive oxygen species (ROS) production, oxidative stress, and inflammation. Additionally, the expression of NF- κ B, caspase-1, and NLRP3 were decreased after pretreatment with ROS scavenging agent *N*-acetylcysteine (NAC, 5 mM pretreated for 2 h) and the NF- κ B nuclear translocation inhibitor Dehydroxymethylepoxyquinomicin (DHMEQ, 10 μ g/mL pretreatment for 4 h) respectively. The results indicate that the activation of the NF- κ B pathway by ROS not only directly promotes the expression of inflammatory factors such as pro-IL-1 β , TNF- α , and IL-6, but also mediates the assembly of NLRP3 by ROS activation of NF- κ B pathway, which indirectly promotes the expression of NLRP3. Finally, a high-degree of overlap between the expression of the NF- κ B and NLRP3 and the activated regions of KCs, further support the importance of KCs in inflammation induced by low-dose CdTe QDs.

1. Introduction

Quantum dots (QDs), are novel semiconductor nanoparticles (NPs), having great applicative value in processes associated with photochemical detection technology and clinical disease diagnosis and medical biological imaging [1–4]. Compared with conventional molecular probes [5], cadmium telluride (CdTe) QDs have advantages of narrow emission spectrum, a wide excitation spectrum, and strong photobleaching resistance [6]. Therefore, they have been widely used in transistors, diode lasers, and as medical imaging agents [7]. The increasingly wide range of applications have resulted in potentially significant increases in human exposure from production to use [8–10]. More importantly, CdTe QDs can easily penetrate biological barriers into the circulation and be transported to the target site. Therefore, it is necessary to evaluate the health risks caused by CdTe QDs.

The liver, as a target of exogenous chemicals, is an important organ involved in substance metabolism [11,12], and has a significantly higher

frequency of interaction with toxins than other organs [13]. Previous studies have shown that the liver is a main accumulation organ allowing NPs to enter the body. NPs are mainly deposited in the liver after exposure, resulting in central vein dilation, focal necrosis, perivascular inflammatory cell aggregation, and abnormal metabolism of liver enzymes [14,15]. Similarly, in *in vitro* studies, local accumulation of NPs occurred in liver cells when they were exposed to NPs at doses far below the lethal dose, and accompanied by a cellular inflammatory reaction and necrosis [16]. Mesoporous silica NPs can cause normal liver cell injury via the NLRP3 inflammasome activation pathway and activation of caspase-1-dependent cell apoptosis [17]. 3-Mercaptopropionic acid capped CdTe QDs (MPA-capped CdTe QDs) can lead to the destruction of the mitochondrial intimal structure, increased intracellular Ca²⁺ levels, decreased mitochondrial membrane potential, and ATP depletion in HepG2 cells [18]. However, it was worth noting that previous studies have mainly focused on liver parenchymal cells and hepatocellular carcinoma cells with malignant proliferation potential as models to

^{*} Corresponding author.

E-mail address: zhangting@seu.edu.cn (T. Zhang).

<https://doi.org/10.1016/j.redox.2021.102157>

Received 5 August 2021; Received in revised form 17 September 2021; Accepted 28 September 2021

Available online 30 September 2021

2213-2317/© 2021 The Authors.

Published by Elsevier B.V. This is an open access article under the CC BY-NC-ND license

(<http://creativecommons.org/licenses/by-nc-nd/4.0/>).

conduct research on hepatotoxicity, but the study of hepatic macrophages with true phagocytic function has rarely received research attention in Kupffer cells (KCs), also known as hepatic macrophages. KCs are special macrophages existing in hepatic sinuses, and account for about 35% of liver nonparenchymal cells. KCs exhibit important biological functions and are the first responders after liver injury [19]. They play a pro-inflammatory role in the early stages of the inflammatory response by recruiting neutrophils, and their anti-inflammatory activity is exerted by capturing apoptotic neutrophils to the late inflammatory stages [20]. Another distinctive reactive property of KCs is their high sensitivity. Compared with members of the non-macrophage family, KCs can produce statistically significant changes in physical and chemical indicators at non-cytotoxic doses, thus assisting in the evaluation of the potential risk of toxic exposure. KCs are a promising *in vitro* model for studying the potential toxicity of xenobiotics at low doses. Nevertheless, based on the limited findings currently available, the functional changes and toxicity mechanisms involved in hepatic macrophages caused by CdTe QDs exposure have yet to be explored in detail.

Exposure to QDs can occur in various ways, including industrial manufacturing, living environments, experimental studies, and medical treatment. QDs can enter the human body through the skin, digestive tract, respiratory tract and vasculature, and can accumulate in the heart, liver, lung and brain [21–23]. While xenobiotics exposed to the skin and digestive tract are generally first subjected to first pass elimination by the liver, following venous exposure to xenobiotics, these can directly enter the blood and have a relatively short stay in the liver, and can quickly exhibit toxic effects. In the recent exposure studies of QDs, high-dose acute exposure is a major issue, but there is a gap between this exposure modality and the characteristics of long-term micro-exposure of the population. Therefore, this study selected 2.5 $\mu\text{M}/\text{kg}$ bw and 10 $\mu\text{M}/\text{kg}$ bw as the lowest-toxic doses that did not cause significant toxic effects (i.e., no accidental deaths of animals occurred during the exposure period and no significant changes in animal body weight in each dose group after exposure, or animal body weight was not reported). In conclusion, the presence of hepatotoxic damage just above the lowest doses, presenting hepatotoxic effects suggests that the risk of exposure to CdTe QDs deserves further evaluation.

Based on the previous literature, QDs are metal-based NPs, with strong ability to induce ROS production [21,24–26]. The oxidative stress reaction involved in ROS is the main mechanism for the toxicity of metal NPs [23,27,28]. In addition, the activation of endoplasmic reticulum stress pathway, lysosomal damage, mitochondrial dysfunction, DNA breakage, and cell cycle disorders are also important mechanisms for the toxic effects of QDs [18,29–31]. For example, exposure to CdTe/ZnS QDs results in inhibition of aerobic respiration, membrane destruction and DNA damage in BV2 cells [32,33]. Further, JB6 cells treated with CdSe QDs, induce G1 phase arrest in cells, and the expression of apoptosis inducing factor (AIF), caspase-6, and caspase-8 were up-regulated [34]. Based on these mechanistic studies, QDs can cause different types of cell damage, but for these damage processes, there seems to be a common initiation stage that dominates the whole reaction process, that is, after cell uptake of QDs, ROS is induced to cause oxidative and antioxidant homeostasis imbalance, which usually acts as the initial trigger for subsequent damage [35].

As a metal-based NPs, QDs exert a strong role in inducing ROS production. Recent studies have found that metal-based NPs lead to different types of damage to liver cells through hierarchical oxidative stress responses. The reaction process includes a disturbance in the body's antioxidant response, a subsequent inflammatory overcompensatory response, and finally cell death after decompensation [36]. Accordingly, the accumulation of ROS caused by QDs exposure may be the main cause of inflammation [29,31,37]. Progression of inflammation can be caused by activation of NLRP3 inflammasomes, although, preconditioning with caspase-1 inhibitors, silencing of NLRP3 expression with NLRP3 siRNA, will significantly reduce the inflammatory response [38]. Currently, the classical activation pathway of NLRP3

is mainly defined as two independent steps [39]. At the initial stage, CdTe QDs and other activators induce the expression of NF- κ B and the mitogen-activated protein kinase-dependent NLRP3 inflammasome. After the activation signal is detected in the activation stage, apoptosis associated speck-like protein containing CARD (ASC) binds NLRP3 protein to the collected pro-caspase, which leads to the activation of pro-caspase-1, and cleavage of its target substrate, pro-IL-1 β , into the mature form. The inflammatory process is finally completed mediated by the inflammasome [27,40]. Furthermore, cadmium-containing QDs can induce normal liver cell inflammation through NLRP3, and the expression of the inflammatory cytokine IL-1 β is associated with the activation of upstream NF- κ B [24,40,41]. Nonetheless, it is still unclear whether the activation of NLRP3 in liver macrophages is associated with ROS production and whether the related inflammatory response mechanism in CdTe QDs induces liver damage.

Considering the knowledge gap about subacute liver effects after exposure to CdTe QDs as well as the role and mechanism of liver macrophage damage induced by CdTe QDs, we conducted *in vitro* and *in vivo* studies to better understand whether low dose CdTe QDs produce toxic effects to the liver during subacute exposure. The results indicated that the expression of the NLRP3 inflammasome in liver macrophages was significantly correlated with the activation of the NF- κ B pathway by ROS, which could be considered as an initiator of the inflammatory response. These results are important to provide a rationale for the countermeasures needed for management of exposure to low doses CdTe QDs in the future, and can be used as a target to control the toxic effects of CdTe QDs.

2. Materials and methods

2.1. Preparation and characterization of CdTe QDs

A tellurium electrode was used as the source of tellurium, and CdTe QDs precursors were formed by Te^{2+} and Cd^{2+} during the electrolysis process. After the electrolysis, the solution was placed in a water bath at 80 °C for 2 h. The duration of the water bath may affect the particle size of the final CdTe QDs. Following the water bath, the samples were stored in a refrigerator at 4 °C for later use. Elution QDs: CdTe QDs were mixed with acetone at a volume ratio of 1:2, centrifuged at 15000 rpm at 4 °C for 20 min. The supernatant was carefully removed and the residual acetone was air-dried in the dark. Then, the CdTe QDs was resuspended with a certain amount of Dulbecco's Modified Eagle's Medium (DMEM) complete medium, which was filtered to remove bacteria using a 0.22 μm filter and were stored at 4 °C in the dark for later use.

The morphology and size of CdTe QDs were determined by transmission electron microscopy (TEM, H-600-4, Hitachi Japan). The excitation wavelength and absorption wavelength of CdTe QDs were measured using a fluorescence spectrophotometer (F-4600, Hitachi, Japan). CdTe QDs were respectively diluted to 20 μM with normal saline and DMEM complete medium, after ultrasonic dispersion for 20 min, the hydrated particle size and zeta potentials of the CdTe QDs in the solution were detected by scanning with a Malvern laser particle size analyzer (Zetasizer NanoZS90, Malvern, England).

2.2. Animals and treatment

Eight-week-old male ICR mice were purchased from Animal Center of Yangzhou University (Yangzhou, Jiangsu, China, NO.20200405016). The animals were housed in standard laboratory conditions according to Jiangsu province guidelines. The animal experiments followed standard procedures for animal housing (20–24 °C, 50–70% humidity, 12-h light and 12-h dark cycles). All procedures involving animals were approved by Experimental animal ethics committee of Southeast University. Before the experiment, we conducted a preliminary experiment to ensure that the dosage set in the *in vivo* experiment would not cause abnormal behavior and physical signs of animals. ICR male mice were

randomly divided into four groups according to weight, and each group included six animals. The mice were intravenously injected (tail vein) once a week for 14 days. In single injection, vehicle control (normal saline), 2.5 $\mu\text{M}/\text{kg}\cdot\text{bw}$ and 10 $\mu\text{M}/\text{kg}\cdot\text{bw}$ of CdTe QDs were given to each mouse, respectively. *N*-acetylcysteine (NAC) (Sigma, USA) was dissolved in normal saline with a concentration of 10 mg/mL, adjusted with NaOH to pH 7.2 to obtain NAC reserve solution. For the last intervention group, on the first day of the experiment, the prepared NAC reserve solution was intraperitoneally injected into mice at the same time every day according to the standard of 100 mg/kg-bw for 14 days, during which the treatment of the intervention group was consistent with 10 $\mu\text{M}/\text{kg}\cdot\text{bw}$ CdTe QDs. At the 14 days after first administration of CdTe QDs, the mice were euthanized to collect blood and liver tissue. Blood biochemical parameters (total protein, albumin, globulin, ALT, AST, and ALP) were determined by Biochemical Autoanalyzer (Type 7170, Hitachi, Japan). Liver tissue was fixed and stained with hematoxylin and eosin (H&E) to examine morphological changes.

2.3. Cell culture and treatment

The mouse Kupffer cell line, KUP5, was purchased from RIKEN Cell Bank (Japan). KUP5 cells were cultured in high-glucose DMEM supplemented with 10% fetal bovine serum (FBS), 10 $\mu\text{g}/\text{mL}$ bovine insulin (Sigma, USA), 250 μM 1-thioglycerol (Sigma, USA), and 100 U/mL/100 $\mu\text{g}/\text{mL}$ penicillin-streptomycin (Gibco, Waltham, MA, USA) at 5% CO_2 and 37 °C. KUP5 cells were cultured until they reached 70–80% confluence before treatment. The exposure doses of CdTe QDs were 0, 5, 50, and 500 nM. Pharmacological inhibitors were included in this study. ROS inhibitor NAC (Beyotime Technology, Shanghai, China) (5 mM for 2 h) and NF- κB nuclear transfer inhibitors DHMEQ (MCE, Shanghai, China) (10 $\mu\text{g}/\text{mL}$ for 4 h) were respectively exposed to KUP5 cells before treatment.

2.4. Cell viability and lactate dehydrogenase assay

A total of 8000 primed KUP5 cells were seeded into each well of a 96-well plate with a total volume of 100 μL . After overnight incubation at 37 °C, the culture media was replaced with CdTe QDs suspensions in DMEM media at concentrations of 0, 5, 50, and 500 nM for 24 h. Then the cytotoxicity was determined using the MTT assay (Sigma-Aldrich, USA) and the Lactate dehydrogenase (LDH) assay (Beyotime Technology, Shanghai, China).

2.5. Determination of intracellular Cd content

To determine intracellular Cd content, KUP5 cells were exposed to 50 nM CdTe QDs for 1.5, 3, 6, 12, and 24 h. The cells were washed with PBS three times, digested with trypsin, and then centrifuged at 1000 rpm for 5 min. The cells were digested in 1 mL of 65% HNO_3 overnight in the dark. The Cd content was measured using atomic absorption spectroscopy (AAS, GFA-7000A, Shimadzu Company, Japan). All measurements were performed in triplicate.

2.6. Observation and quantification of intracellular reactive oxygen species

KUP5 cells (5×10^4) were cultured in 2 mL in wells of a 6-well plate and incubated with 0, 5, 50, and 500 nM CdTe QDs for 24 h. Intracellular ROS levels were measured using fluorescence microscopy (VERT.A1, ZEISS AG, Germany) and flow cytometry (FACSCANTO II, BD Bioscience) using the Reactive Oxygen Species Assay Kit (Beyotime Technology, Shanghai). In brief, KUP5 cells exposed to CdTe QDs for 24 h were washed with PBS twice, then diluted with serum-free medium and DCFH-DA at a ratio of 1:2000 and incubated at 37 °C for 30 min. Finally, the fluorescence signal could be photographed after cleaning with PBS. The laser axis positioned at an angle of about 90° with a laser beam is

called side scattered light (SSC), and the size of SSC is proportional to the complexity of the particle composition of the cell. The fluorescence values of the SSC and DCF in different dose groups were normalized to evaluate the production of intracellular ROS and the uptake of intracellular particulate matter. The excitation wavelength and emission wavelengths were 488 nm and 525 nm, respectively. The data was evaluated using FlowJo, version 10.4.

2.7. Western blotting analysis

KUP5 cells (5×10^4) were cultured in a volume of 2 mL complete medium in the wells of a 6-well plate overnight and incubated with 0, 5, 50, and 500 nM CdTe QDs for 24 h. Next, the cells were washed twice with PBS and 50 μL of RIPA Lysis Buffer (Beyotime, Shanghai, China) and 0.5 μL PMSF (Beyotime, Shanghai, China) was added to each well. The protein lysate was incubated on ice for 30 min and then centrifuged for 10 min (12000 rpm, 4 °C). The protein supernatant was placed in a new centrifuge tube and stored on ice. The concentration of the protein samples was quantified using the BCA protein assay kit (EpiZyme, Shanghai, China) and aliquots containing equal amount of proteins were resolved by SDS-PAGE in sample loading buffer and transferred to 0.2 μm PVDF membranes. Next, the membranes were washed with TBST 3 times for 10 min each. Finally, the membranes were trimmed and incubated overnight at 4 °C with diluted primary antibodies. ECL luminous solution (Thermo Fisher Scientific, USA) was prepared as a 1:1 solution, and proteins were detected. The primary antibodies used in this study included anti-NF- κB , anti-NLRP3, anti-I κB , anti-pro-IL-1 β +IL-1 β , and anti-GAPDH (all from ABclonal Technology, Wuhan, China) and anti-pro caspase-1 + p10 + p12 (Abcam, UK).

2.8. ELISA

KUP5 cells (5×10^4) were cultured in 2 mL medium in the wells of a 6-well plate overnight and were incubated with 0, 5, 50, and 500 nM CdTe QDs for 24 h. Next, the supernatants were collected to determine the levels of the pro-inflammatory cytokines IL-1 β , TNF- α , and IL-6 using ELISA kits according to manufacturer's instructions (Yi Fei Xue Biotechnology, Nanjing, China). Concentrations were expressed as picograms per milliliter (pg/mL).

2.9. Tissue immunochemical staining

Paraffin slices of liver tissue were dewaxed, repaired by antigen and blocked by endogenous peroxidase (refer to the Supporting Experimental Section for specific steps), and sealed with 3%BSA at room temperature for 30min. Liver tissue slices were incubated with primary antibody, and 1:100 diluted primary antibody was incubated overnight at 4 °C: TNF- α , IL-1 β , IL-6, NF- κB , NLRP3 and F4/80 (ABclonal Technology, Wuhan, China). Secondary antibody was incubated at 37 °C for 30min or room temperature for 50min. After DAB chromogenic and nucleus counterstaining, the slices were sealed with neutral gum and observed under a microscope. The positive area was brownish yellow. Quantified using the image processing software ImageJ1.53a.

2.10. Statistical analysis

The quantifiable experimental results are reported as the mean and standard deviation (SD) of three independent experiments ($n = 3$). SPSS Statistical software version 23.0 was used for statistical analysis. One-way ANOVA was used to determine if the statistical difference between the control and the exposure group was statistically significant, and then the Tukey LSD (Least Significant Difference) *post-hoc* test was used to determine whether the differences between the groups was statistically significant. Finally, *P*-values <0.05 or <0.01 were considered statistically significant.

3. Results

3.1. Physical characterization of CdTe QDs

The morphology and size of CdTe QDs were observed by TEM. As shown in Fig. 1A and B, the CdTe QDs were well-dispersed, the particle size of CdTe QDs was mainly distributed between 2.2 and 3.0 nm. The maximum excitation and emission wavelength of CdTe QDs were 300 nm and 570 nm, respectively (Fig. 1C). According to Table 1, the hydration particle size and zeta potential of CdTe QDs in normal saline and DMEM medium were 4.06 ± 1.09 nm and 8.94 ± 0.69 nm, -5.84 ± 1.80 mV and -9.02 ± 0.66 mV, respectively.

3.2. Liver damage and inflammation in mice induced by CdTe QDs

We determined the dose for the *in vivo* experiment according to the previous pre-experiment. Mice showed no significant weight change at the set dose ($P > 0.05$) (Fig. S1). Analysis of liver coefficient of mice treated with CdTe QDs showed that although there was no abnormality in low-dose (2.5 $\mu\text{M}/\text{kg}\cdot\text{bw}$) exposure, liver coefficient of mice exposed to high-dose (10 $\mu\text{M}/\text{kg}\cdot\text{bw}$) increased significantly ($P < 0.05$) (Fig. S2). To determine whether CdTe QDs caused liver damage, we first observed changes in blood biochemical parameters caused by CdTe QDs. As shown in Fig. 2A, following CdTe QDs administration, the levels of AST in the blood increased in a dose-dependent manner with the increasing dose in mice ($P < 0.05$). In addition, liver samples collected from CdTe QDs-treated animals showed several morphological changes. Liver tissues presented vacuolation and reduced cell pseudopods, partial nuclear fragmentation, and loss, a small amount of inflammatory cells infiltrated around the blood vessels and a small amount of exudate filled the hepatic duct, especially in the 10 $\mu\text{M}/\text{kg}\cdot\text{bw}$ treatment group (Fig. 2B). Subsequently, the oxidative stress markers were evaluated to further determine changes in liver injury. As shown in Fig. 2C and D, compared with the control group, the protein expression of Nrf2 and HO-1 was significantly increased ($P < 0.05$). Fig. 2E illustrates the activation of macrophages in the liver tissue of mice following exposure to CdTe QDs. The activated macrophages mostly migrated in the space of liver cells, and the morphology was more irregular and smaller than that of normal liver cells. Activated positive tan areas were observed in the low-dose treatment group. In addition, the expression of inflammatory cytokines IL-1 β , TNF- α , and IL-6 was significantly increased on liver tissue immunohistochemistry compared with the control group ($P < 0.05$) (Fig. 2F). This evidence demonstrated that CdTe QDs induced liver injury in mice, which was closely related to the CdTe QDs-induced oxidative stress and inflammatory activity in liver. Furthermore, hepatic macrophages were activated after CdTe QDs treatment, while the activation process may be related to the triggering of the subsequent inflammatory response.

3.3. Cytotoxicity, intracellular uptake and ROS production caused by CdTe QDs in KUP5 cells

Cytotoxicity assessment was used to conduct cell viability assays and the LDH assay on the CdTe QDs. As shown in Fig. 3A and B, KUP5 cells were treated with 5–500 nM CdTe QDs for 24 h and dose-dependent toxicity for CdTe QDs was observed. When the concentration of CdTe QDs was 500 nM, the cell viability of KUP5 cells was reduced by 50%. However, there was no significant decrease in cell viability at the lower dose of 5 nM. Interestingly, the cell membrane damage of KUP5 cells observed at the doses of 5 and 500 nM resulted in significant changes in LDH release ($P < 0.05$). Furthermore, with increasing exposure to the doses, the number of cells gradually decreased, and the cell morphology was altered. As the cell's pseudopods shortened (Fig. 3C). Based on the toxicity profiles of CdTe QDs, we hypothesized that intracellular uptake of CdTe QDs may contribute to their toxicity, and AAS analysis was used to quantify the Cd content of CdTe QDs particles in cells (Fig. 3F). We selected a dose of 50 nM, a dose in which the cell membrane was not seriously damaged. At this dose, the content of Cd in cells gradually increased as the exposure time increased, and the levels of Cd in cells reached a maximum at 12 h and 24 h after exposure. Since the mechanism of CdTe QDs-induced toxicity may involve oxidative stress that may derive from intracellular uptake, we evaluated intracellular ROS levels using fluorescence microscopy and the ROS were quantified by flow cytometry. As shown in Fig. 3C, D and 3F, the fluorescence intensity of cells in the 500 nM dose group was the highest and was consistent with the LDH results. The consistency between LDH and ROS accumulation led us to speculate that the aggravation of membrane damage may result from the uptake of higher levels of CdTe QDs, and thus a stronger ROS accumulation. To this end, we analyzed the correlation between cell uptake and ROS by flow cytometry. When combined with Fig. 3G and H, it can be found that the correlation between intracellular particle intake and ROS is more obvious in the medium-high dose group. As shown in Fig. 3G, it can be seen more intuitively that the percentage in Q2 quadrant gradually increases with the increase of dose, indicating that cells with more intracellular particles intake are more inclined to stimulate stronger ROS production [42,43].

3.4. CdTe QDs stimulated high expression of the NLRP3 inflammasome, activation of NF- κ B, and secretion of inflammatory cytokines in KUP5 cells

To further explore the levels of cellular inflammation, the content of intracellular inflammatory cytokines and the expression of inflammation-related pathway proteins were measured. The release of key inflammatory cytokines IL-1 β , TNF- α , and IL-6 in cell supernatant was detected by ELISA and the results showed a trend with increasing dose (Fig. 4A). To prevent treatment with a high dose of 500 nM CdTe QDs (survival rate of 50%), three doses of 0, 5, and 50 nM were selected

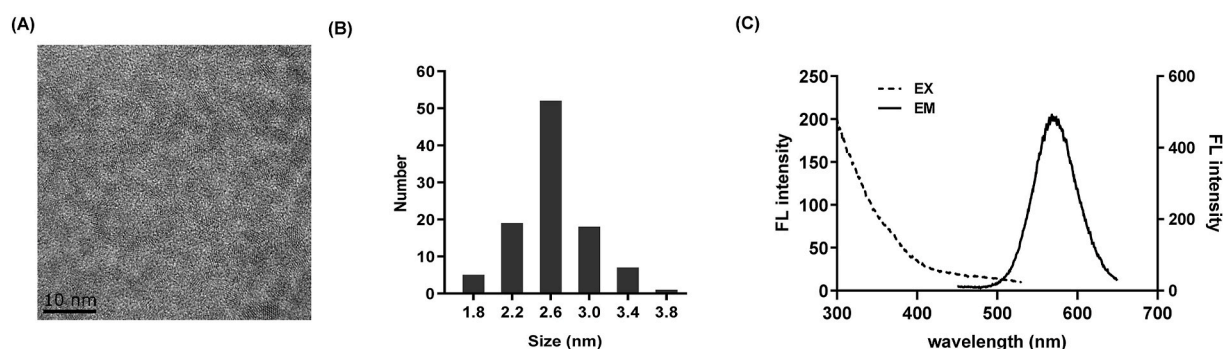


Fig. 1. Physical characterization of CdTe QDs. (A) Transmission electron microscope imaging. (B) The particle size distribution. (C) Excitation (dotted line) and emission (solid line) spectra of CdTe QDs in water.

Table 1
Hydration particle sizes and zeta potentials of CdTe QDs in different systems.

Indicators	Hydrodynamic diameter (nm)		Zeta potential (mV)	
	Normal saline	DMEM	Normal saline	DMEM
Values (Mean \pm SD)	4.06 \pm 1.09	8.94 \pm 0.69	-5.84 \pm 1.80	-9.02 \pm 0.66

DMEM: Dulbecco's Modified Eagle's Medium (DMEM) complete medium. Repeat three times.

for the mechanism study in subsequent experiments. The NF- κ B pathway plays a key role in the inflammatory response mediated by oxidative stress. In addition, NLRP3 is a protein closely related to inflammation, and its expression level can directly reflect the body's inflammation level. The western blotting results are shown in Fig. 4B and C. As the concentration of CdTe QDs increased, the expression of NF- κ B increased significantly. At the same time, the expression of the inhibitory protein I κ B- α of NF- κ B was down-regulated. IL-1 β is a key inflammatory factor downstream of the NF- κ B pathway and is involved in the regulation of inflammatory response, and can in turn reflect inflammatory changes. NLRP3 and caspase-1 are important components that constitute the NLRP3 inflammasome complex. The results showed that the expression levels of NLRP3 and mature caspase-1 revealed a consistent upward trend, while the expression of the precursor protein pro-caspase-1 of mature caspase-1 was just the opposite. These results indicated that the inflammatory response of KUP5 cells was significantly increased after CdTe QDs processing, including the activation of NF- κ B pathway and the expression of NLRP3. In addition, an important finding was that even low doses (5 nM) of CdTe QDs could trigger the activation of inflammatory pathway.

3.5. NAC reduced the secretion of inflammatory cytokines, inhibited the expression of NLRP3 and the activation of NF- κ B by reducing ROS production

Previous studies have shown that CdTe QDs can indeed induce oxidative stress and inflammatory responses in KUP5 cells, but the exact mechanism has not been clarified. ROS can act as an activator of oxidative stress. Therefore, in order to explore whether ROS is involved in CdTe QDs-induced oxidative stress and the inflammatory response, this study designed a NAC preconditioning group. We first determined the effect of NAC pretreatment on KUP5 cell viability (Fig. S3), and the results showed that NAC alone did not cause significant cell toxicity. Subsequently, intracellular ROS levels were determined after NAC pretreatment. Fig. 5A shows that the morphology and number of KUP5 cells tended to be normal after ROS removal, which demonstrated that CdTe QD treatment resulted in ROS production, and ROS levels may be involved in the activation of a subsequent inflammatory responses. To further evaluate the role of ROS on the inflammatory response, the levels of the inflammatory cytokines IL-1 β , TNF- α , and IL-6 in the supernatant of KUP5 cells were measured by ELISA (Fig. 5B). The results showed that the levels of inflammatory cytokines decreased following ROS removal. Further, there was a correlation between the accumulation of ROS caused by CdTe QDs and the inflammatory response. We tested the relationship between ROS levels and the NF- κ B pathway and NLRP3 expression in the inflammatory response, and the related proteins were determined by western blotting (Fig. 5C and D). Following ROS clearance using the scavenger NAC, the expression of NF- κ B and NLRP3 decreased. In addition, the expression of caspase-1 and IL-1 β were also decreased. These results suggested that ROS was involved in the inflammatory response induced by CdTe QDs, and the activation of NF- κ B pathway and the high expression of NLRP3 played an important role in the ROS-activated inflammatory response.

3.6. The ROS/NF- κ B pathway was involved in the secretion of inflammatory cytokines and the expression of the NLRP3 inflammasome induced by CdTe QDs

To further investigate whether activation of the NF- κ B pathway in the presence of ROS influences the expression of the NLRP3 inflammasome, we used DHMEQ, an irreversible nuclear transport inhibitor of NF- κ B, to pretreat KUP5 cells. ELISA results showed that after DHMEQ pretreatment, the content of inflammatory cytokines in the cell supernatant was decreased (Fig. 6A). Western blotting results are shown in Fig. 6B and C. DHMEQ significantly inhibited the nuclear translocation of NF- κ B, decreased the expression of NF- κ B, and down-regulated the expression of Pro-IL-1 β downstream of the NF- κ B pathway. In addition, the expressions of NLRP3 and caspase-1 were also decreased, suggesting that the NF- κ B pathway may regulate the expression of NLRP3 by affecting the initiate of the NLRP3 inflammatory complex. The formation of caspase-1 comes from the recruitment, processing, and activation of pro-caspase-1. As the expression of pro-caspase-1 increased, the final expression level of caspase-1 decreased. This suggested that NF- κ B might also affect the formation of the NLRP3 inflammasome complex by influencing the recruitment of pro-caspase-1. In addition, caspase-1 acted as an IL-1 β invertase, suggesting that the low expression of IL-1 β was associated with the down-regulation of caspase-1. These results suggested that the NF- κ B pathway might affect the expression of NLRP3 through multiple channels in the ROS-activated inflammatory response.

3.7. NAC decreased the secretion of inflammatory factors and alleviated the liver toxicity in mice induced by CdTe QDs

As can be seen from the results of the NAC pretreated mice, liver damage indexes ALT, AST, and ALP in the serum of pretreated mice were decreased (Fig. 7A), and the expression of antioxidant proteins Nrf2 and HO-1 in liver tissue were decreased (Fig. 7B and C), indicating that NAC alleviated the oxidative stress induced by CdTe QDs in mice. The results of the immunohistochemistry indicated that the expressions of three inflammatory factors, IL-1 β , TNF- α , and IL-6 were decreased in the liver tissues of mice in the pretreatment group ($P < 0.05$) (Fig. 7E). At the same time, combined with the pathological sections of liver tissue, the inflammatory infiltration of mice in the pretreatment group was reduced and tissue vacuolization was alleviated (Fig. 7B). The immunohistochemical results of NF- κ B and NLRP3 were successful in confirming the alleviation of liver inflammation after ROS clearance (Fig. 7F) and the reduced activation percentage of liver macrophages after NAC pretreatment (Fig. 7G). More importantly, this study observed a high degree of overlap between regions with high NLRP3 expression and regions with NF- κ B activation and regions activated by hepatic macrophages, suggesting that the activation of hepatic macrophages may be involved in the CdTe QDs-induced oxidative stress and inflammatory response, and there is a certain correlation between the expression of NLRP3 and the activation of NF- κ B in the oxidative response.

4. Discussion

This study evaluated the risk of CdTe QDs exposure based on *in vivo* and *in vitro* experiments. We revealed the effects of CdTe QDs-induced liver injury *in vivo* and further verified the mechanisms of injury *in vitro*. The *in vivo* studies demonstrated that subacute CdTe QDs treatment could lead to an imbalance of antioxidant, inflammatory infiltration and abnormal changes in liver metabolic enzymes. The *in vitro* results were consistent with oxidative damage and inflammation in the liver after 14 days of tail vein exposure of CdTe QDs, which also induced higher ROS generation, resulting in the accumulation of inflammatory cytokines IL-1 β , TNF- α and IL-6. *In vitro* studies also suggested that the mechanism of CdTe QDs induced injury may involve the assembly of NLRP3 inflammasome and activation of the NF- κ B pathway. Collectively, these data indicated that, NLRP3 inflammasome expression in

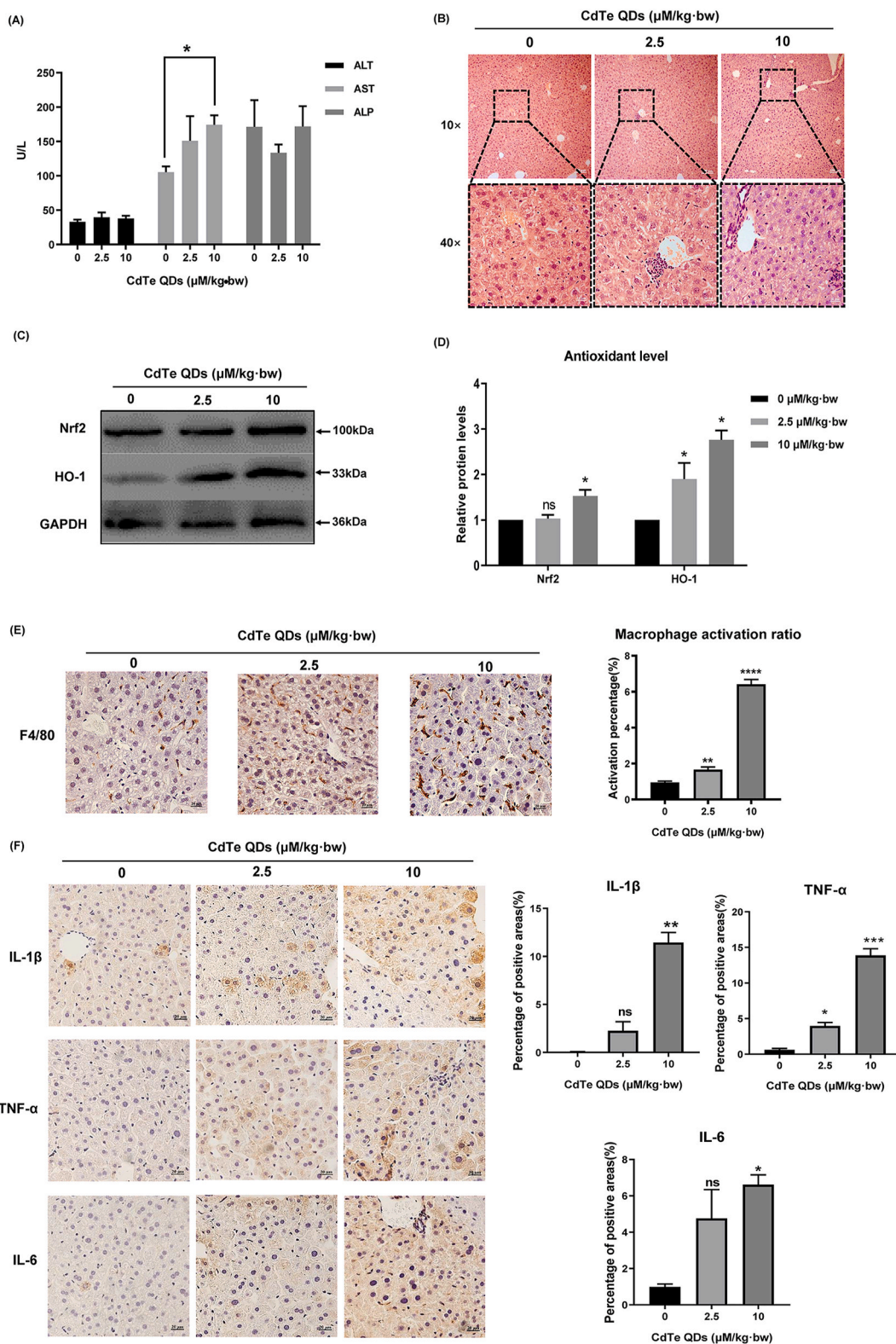
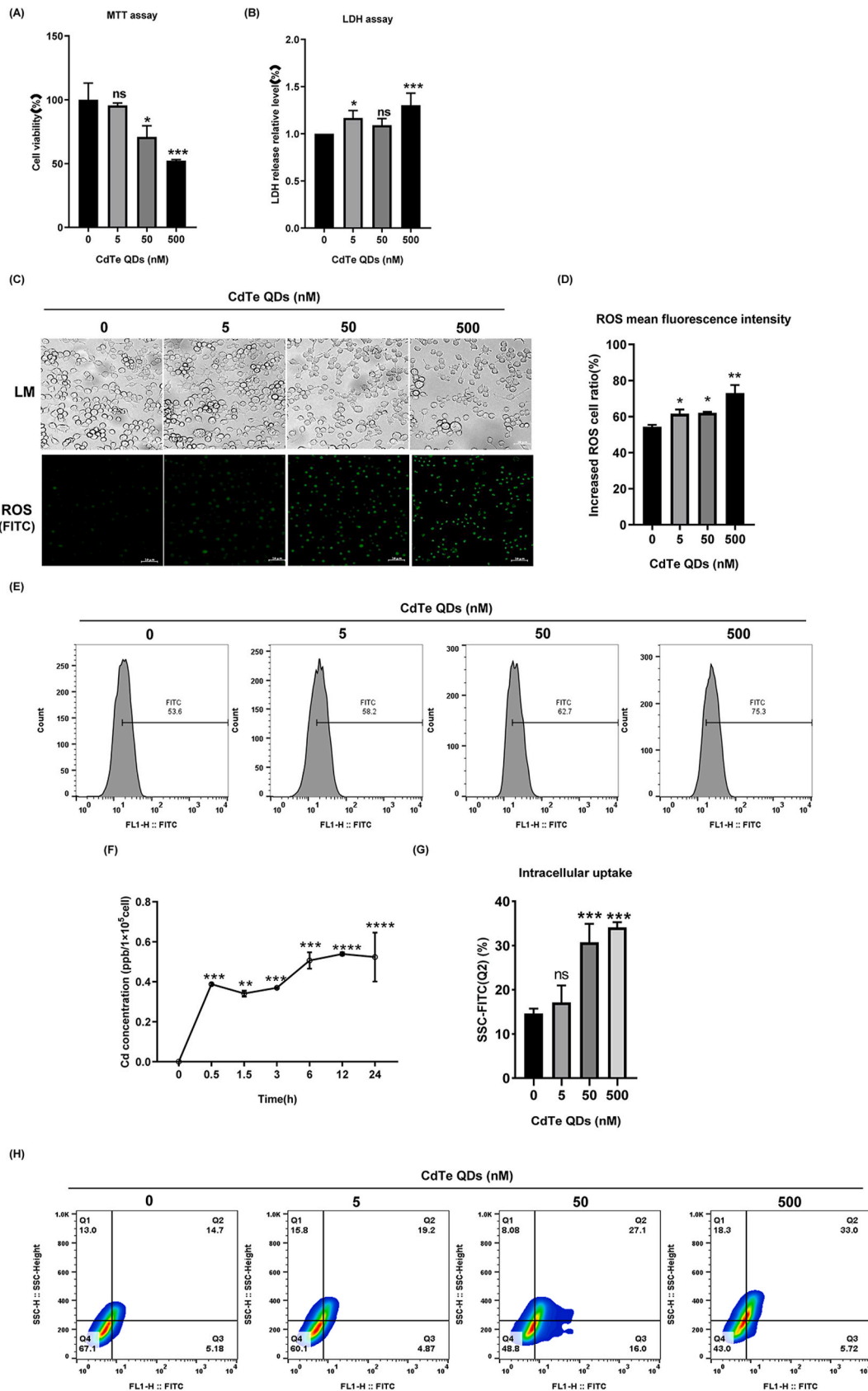


Fig. 2. Liver damage and inflammation in mice caused by CdTe QDs. (A) Serum levels of ALT, AST, and ALP after mice were treated with low (2.5 μM/kg-bw) and high (10 μM/kg-bw) doses of CdTe QDs for 14 days. n = 6 male mice for each group. (B) The pathological changes of liver tissues of mice treated with different doses of CdTe QDs after 14 days (HE staining). n = 6 male mice for each group. Magnification using 10 × and 40 × objectives, bar scale = 100 μm and 20 μm respectively. Qualitative (C) and quantitative (D) evaluation of the expression of antioxidant related proteins Nrf2 and HO-1 in liver tissue of mice treated with different doses of CdTe QDs after 14 days. n = 6 male mice for each group. (E) Activated hepatic macrophages were labeled by F4/80. n = 6 male mice for each group. Magnification = 400 ×, bar scale = 20 μm. (F) Immunohistochemical expression of IL-1β, TNF-α, and IL-6 in liver tissue of mice treated with different doses of CdTe QDs for 14 days. n = 6 male mice for each group. Magnification = 400 ×, bar scale = 20 μm. All values are mean ± SD. The statistical significance of differences was evaluated by one-way ANOVA. ns, P > 0.05; *P < 0.05; **P < 0.01, ***P < 0.001; ****P < 0.0001 for all conditions. All the above are compared with the control group.



(caption on next page)

Fig. 3. Cytotoxicity, intracellular uptake, and ROS production caused by CdTe QDs in KUP5 cell. (A) MTT assay of KUP5 treated with different concentrations of CdTe QDs (0, 5, 50, or 500 nM) for 24 h $n = 3$ replications. (B) Degree of membrane lipid peroxidation of KUP5 after 24 h treatment with different concentrations of CdTe QDs. $n = 3$ replications. (C) Cell morphology changes of KUP5 cells treated with different doses of CdTe QDs for 24 h. ROS generation was observed by fluorescence microscopy (in green). Magnification = $400\times$, bar scale = $20\ \mu\text{m}$ $n = 3$ replications. (D) and (E) show the relative fluorescence intensity of intracellular ROS in KUP5 cells treated with different doses of CdTe QDs for 24 h measured by Flow Cytometry. $n = 3$ replications. (F) Cadmium content in KUP5 cells treated with 50 nM CdTe QDs for 0, 0.5, 1.5, 3, 6, 12, and 24 h was determined by the AAS method. $n = 3$ replications. (G) and (H) show the intracellular particle uptake of KUP5 cells treated with different concentrations (0 nM, 5 nM, 50 nM, 500 nM) of CdTe QDs for 24 h $n = 3$ replications. All values are mean \pm SD. The statistical significance of differences was evaluated by one-way ANOVA. ns, $P > 0.05$; *, $P < 0.05$; **, $P < 0.01$; ***, $P < 0.001$. All the above are compared with the control group. (For interpretation of the references to colour in this figure legend, the reader is referred to the Web version of this article.)

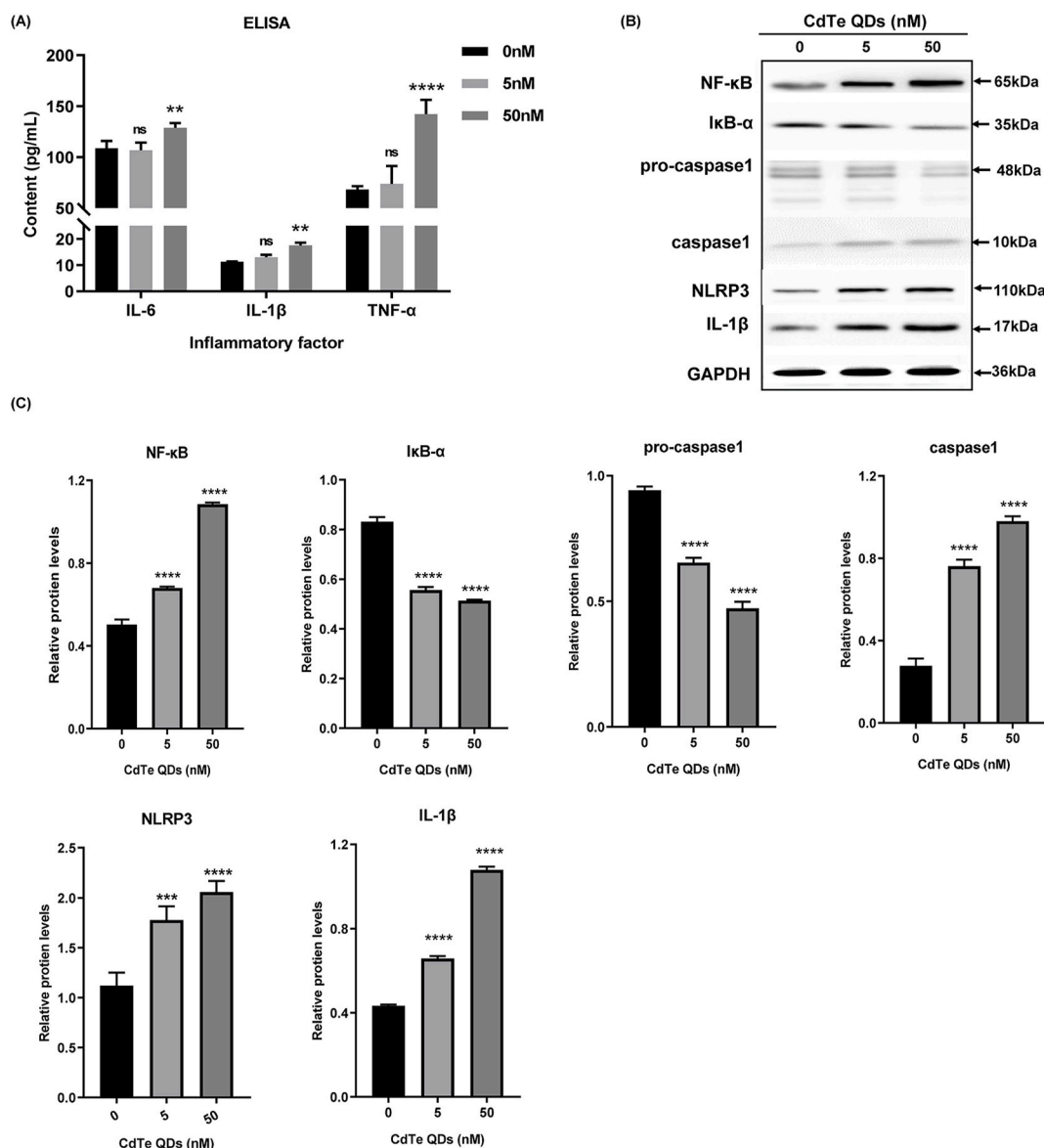


Fig. 4. CdTe QDs stimulate the activation of the NLRP3 inflammasome, phosphorylation of NF- κ B, and secretion of inflammatory factors in KUP5 cells. (A) The contents of inflammatory factors IL-1 β , TNF- α , and IL-6 in the supernatant of KUP5 cells treated with 0, 5 and 50 nM CdTe QDs for 24 h were determined by ELISA. $n = 4$ replications. (B) and (C) show the protein expression of NF- κ B, I κ B, pro-caspase-1, caspase-1, NLRP3, and IL-1 β in KUP5 cells treated with 0, 5, and 50 nM CdTe QDs for 24 h as measured by western blotting. $n = 3$ replications. All values are mean \pm SD. The statistical significance of differences was evaluated by one-way ANOVA. ns, $P > 0.05$; *, $P < 0.05$; **, $P < 0.01$; ***, $P < 0.001$; ****, $P < 0.001$. All the above are compared with the control group.

liver macrophages was significantly correlated with the activation of NF- κ B pathway involved by ROS, which could be used as the initiator of the inflammatory response. This study provides countermeasures for coping with the exposure risk caused by CdTe QDs in the future, and can be used as a molecular target identified may be used to control the toxic effects of CdTe QDs.

After absorption by the body, CdTe QDs can accumulate in the liver

[44]. Liver can be used as the primary target after intravenous injection of nanomaterials and as a secondary target after environmental exposure of nanomaterials [45]. Thus, our study then established an *in vivo* model of low-level QDs tail vein exposure, focusing on the liver tissue damage caused by CdTe QDs. KUP5 cells are a kind of immune cells mainly distributed in hepatic sinusoids, which have the advantage of early response to xenobiotics in blood. Based on previous studies on

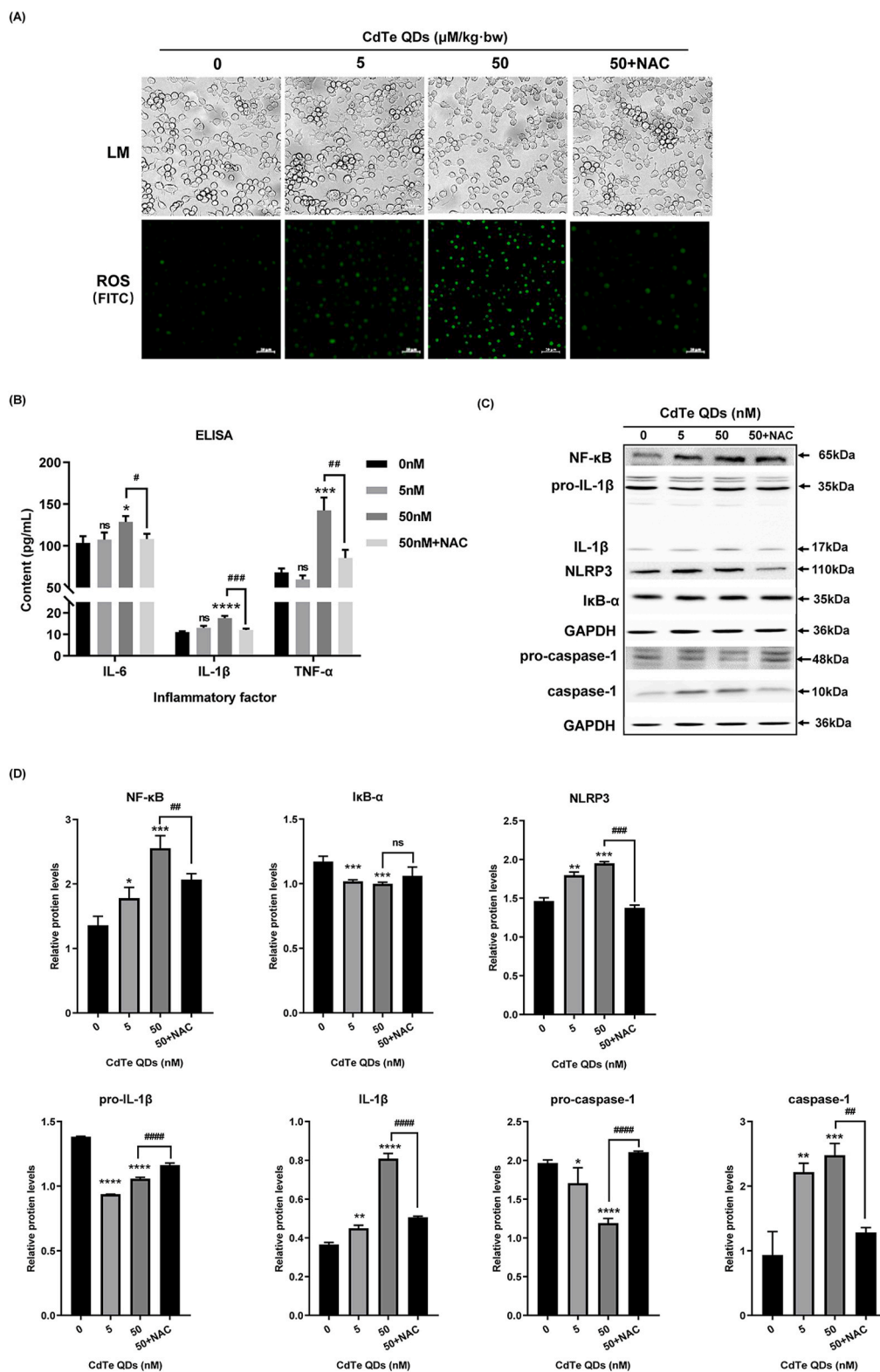


Fig. 5. Effects of NAC preconditioning on the expression of inflammatory factors and NF-κB pathway proteins in KUP5 cells. KUP5 cells were pretreated with NAC (5 mM) for 2 h and then were treated with CdTe QDs (50 nM) for 24 h(A) Cell morphology changes of KUP5 cells after treatment with CdTe QDs. ROS generation was observed by fluorescence microscopy (in green). n = 3 replications. (B) The levels of inflammatory factors IL-1β, TNF-α, and IL-6 in the supernatant of KUP5 cells treated with CdTe QDs for 24 h were determined by ELISA. n = 4 replications. (C) and (D) show the protein expression of NF-κB, IκB, pro-caspase-1, caspase-1, NLRP3, IL-1β, and pro-IL-1β in KUP5 cells treated with CdTe QDs for 24 h by western blotting. n = 3 replications. All values are mean ± SD. ns, $P > 0.05$; *, $P < 0.05$; **, $P < 0.01$; ***, $P < 0.001$; ****, $P < 0.0001$; All the above are compared with the control group. Compared to the 50 nM dose group: #, $P < 0.05$; ##, $P < 0.01$; ###, $P < 0.001$; ####, $P < 0.0001$.

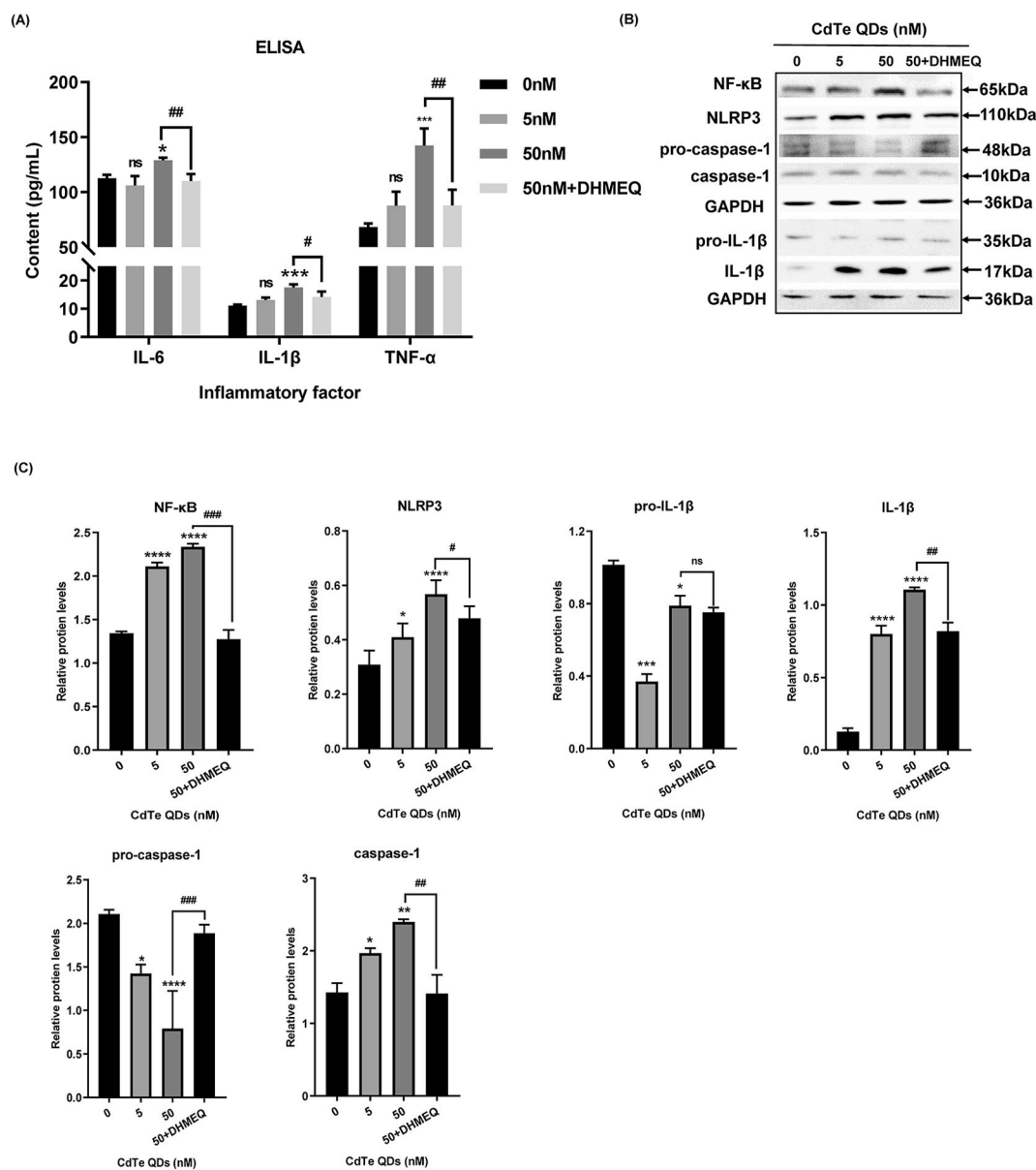


Fig. 6. Effects of DHMEQ pretreatment on the expression of inflammatory factors and NF- κ B pathway proteins in KUP5 cells after 24 h exposure to CdTe QDs. KUP5 cells were pretreated with DHMEQ (10 μ g/mL), an irreversible inhibitor of nuclear translocation of NF- κ B, for 4 h and then treated with CdTe QDs (50 nM) for 24 h. (A) The levels of inflammatory factors IL-1 β , TNF- α and IL-6 in the supernatant of KUP5 cells treated with CdTe QDs for 24 h as determined by ELISA. $n = 4$ replications. (B) and (C) show the protein expression of NF- κ B, pro-caspase-1, caspase-1, NLRP3, IL-1 β , and pro-IL-1 β in KUP5 cells treated with CdTe QDs for 24 h by western blotting. $n = 3$ replications. All values are mean \pm SD. The statistical significance of differences was evaluated by one-way ANOVA. ns, $P > 0.05$; *, $P < 0.05$; **, $P < 0.01$; ***, $P < 0.001$; ****, $P < 0.0001$; All the above are compared with the control group. Compared to the 50 nM dose group: #, $P < 0.05$; ##, $P < 0.01$; ###, $P < 0.001$; ####, $P < 0.0001$.

CdTe QDs hepatotoxicity, KUP5 cells revealed higher sensitivity. For all types of hepatocytes, when the exogenous particles are transported to the liver through the blood, they are first recognized and engulfed by hepatic macrophages located near the hepatic sinusoids, causing damage to the liver macrophages. On one hand, it will significantly reduce the liver's ability to remove foreign bodies. On the other hand, hepatic macrophages after injury can stimulate oxidative stress and inflammatory responses, which indirectly cause liver cell damage. In the low-dose exposure set in this study, we speculated that KUP5 cells would be significantly activated. As a result, *in vivo* experiments firstly focused on the activation of KUP5 cells by exposure to low-dose CdTe QDs, and then analyzed the mechanism of oxidative damage and inflammatory factor release induced by low-dose CdTe QDs. In addition to the digestive functions of protein synthesis and transport, carbohydrate metabolism,

and the transfer of lipid components such as cholesterol, the liver also exerts immune defense functions such as assisting the removal of endotoxins and regulating innate immunity [36]. In the process of the liver participating in the metabolism of nutrients in the body, the participation of liver metabolic enzymes cannot be ignored, which can indirectly reflect whether the liver function is normal or not. In this study, AST levels of the high-dose group were significantly increased, and cell vacuolation, whereby liver cell injury causes cell swelling, cytoplasmic looseness, intracellular vacuolation and "balloon-like change", and inflammatory cell infiltration of the liver tissue could be intuitively observed in the pathological sections. The pathological damage gradually progresses and deteriorates, and eventually affects the normal physiological function of liver cells [46]. In order to clarify whether oxidative stress and inflammatory changes are involved in liver tissue

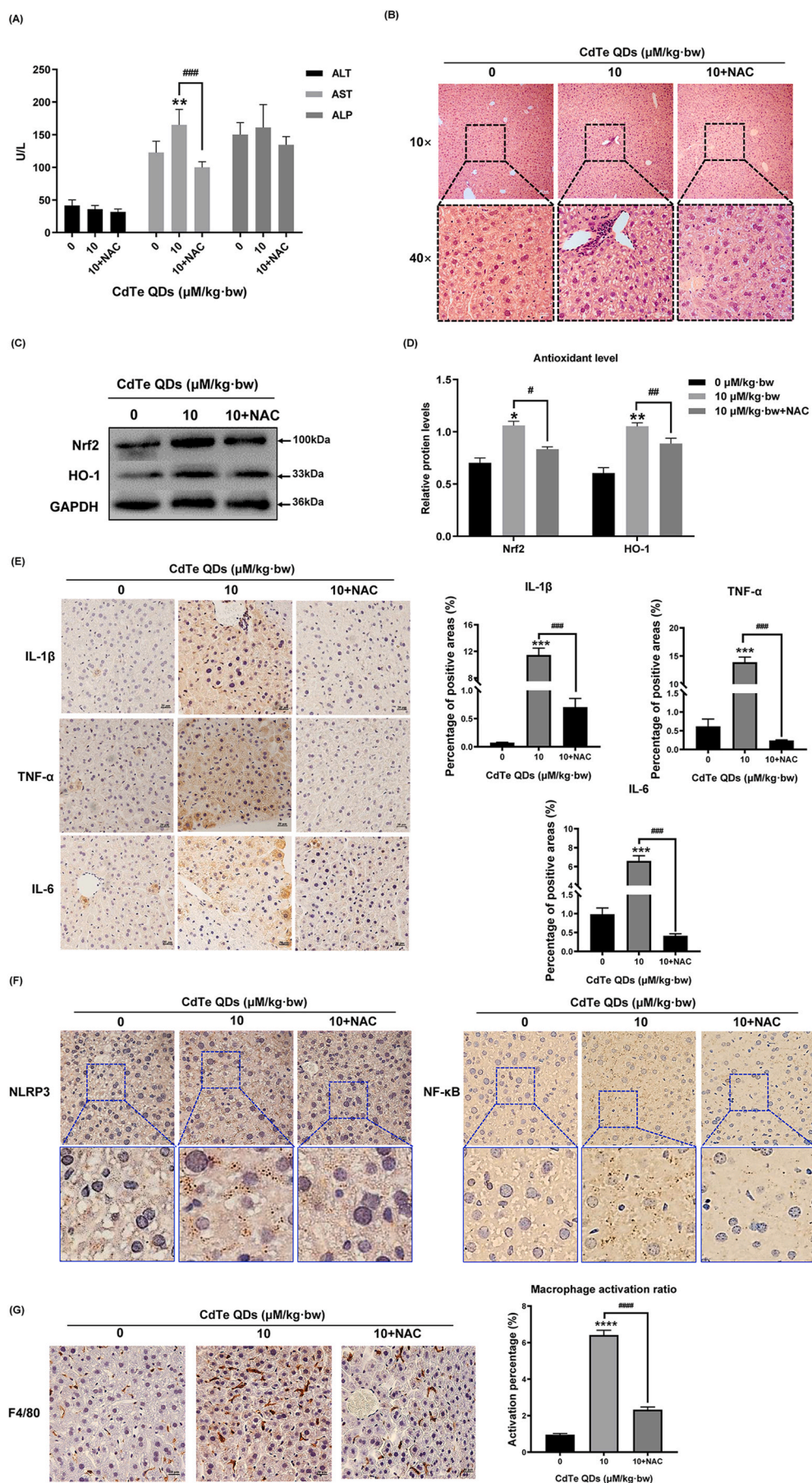


Fig. 7. NAC decreased the secretion of inflammatory factors and alleviated the liver toxicity in mice induced by CdTe QDs. Mice were pretreated by intraperitoneal injection of NAC (100 mg/kg-bw) for 2 h, and then exposed to CdTe QDs (10 μM/kg-bw) via the tail vein for 14 days. (A) Serum levels of ALT, AST, and ALP after mice treatment with CdTe QDs in the low dose (2.5 μM/kg bw), high dose (10 μM/kg-bw), and NAC pretreatment groups (10 μM/kg-bw + NAC) for 14 days. n = 6 male mice for each group. (B) Pathological damage to liver tissue after NAC pre-treatment. n = 6 male mice for each group. Magnification using 10 × and 40 × objectives, bar scale = 100 μm and 20 μm respectively. (C) and (D) Expression of antioxidant related proteins Nrf2 and HO-1 in liver tissue of NAC-pretreated mice after 14 days of 10 μM/kg-bw CdTe QDs treatment. n = 6 male mice for each group. (E) Immunohistochemical results of IL-1β, TNF-α, and IL-6 in liver tissue of NAC pretreated mice. n = 6 male mice for each group. Magnification = 400 ×, bar scale = 20 μm. (F) The expression levels of NF-κB and NLRP3 in the liver tissues of NAC pretreated mice were evaluated by immunohistochemistry. n = 6 male mice for each group. Magnification = 400 ×, bar scale = 20 μm. (G) Activated macrophages in mouse liver tissues pretreated with NAC were labeled by F4/80. n = 6 male mice for each group. Magnification = 400 ×, bar scale = 20 μm. All values are mean ± SD. The statistical significance of differences was evaluated by one-way ANOVA. *, $P < 0.05$; **, $P < 0.01$; ***, $P < 0.001$; ****, $P < 0.0001$. All the above are compared with the control group. Compared to the 10 μM/kg-bw dose group: #, $P < 0.05$; ##, $P < 0.01$; ###, $P < 0.001$.

injury, the expression of key proteins HO-1 and Nrf2 and the expression of inflammatory cytokines IL-1 β , TNF- α , and IL-6 in liver tissue were subsequently measured. Under normal physiological conditions, HO-1 protein expression levels and reactivity were relatively low. However, under the stimulation of xenobiotics, its upstream transcription factor Nrf2 first separates from its inhibitor protein Keap-1, then the phosphorylated Nrf2 can avoid being degraded by ubiquitination and thus enters the nucleus to form heterodimer with Maf protein, and finally binds with ARE to initiate HO-1 expression [47]. In this study, the increased expression of antioxidant protein HO-1 was consistent with changes in the upstream transcription factor Nrf2, which indicated that the subacute treatment of low dose CdTe QDs could cause an imbalance between oxidation and antioxidation in the liver tissue of mice [48,49]. This reaction process is consistent with Tier2 in the three-tiered sequence proposed by Nel et al. [50]. After the initial antioxidant defense response in Tier 1, the organism transitions to the Tier 2 stage, which represents a stage of antioxidant defense failure, and thus, a large amount of ROS accumulates and causes intense oxidative stress and inflammation. Furthermore, as a defense against liver injury, mobilization of hepatic macrophages is usually the primary cell response. To this end, activated macrophages were labeled with F4/80, and the results showed that hepatic macrophages were activated synchronously and concentrated in the intercellular space during liver injury. Furthermore, our *in vivo* study also showed a high expression of inflammatory cytokines IL-1 β , TNF- α , and IL-6 after low-dose CdTe QD treatment. The above provide evidence to support the hypothesis that liver injury is caused by sub-acute exposure to low-dose CdTe QDs. CdTe QDs are recognized by macrophages and result in an imbalance of oxidation and antioxidation reactions in the body through the activation of macrophages, which then lead to local inflammatory damage through excessive oxidative stress.

Given the association between the activation of liver macrophages and inflammatory damage after low dose CdTe QDs treatment, this study successfully established an *in vitro* model using KUP5 cells to further explore the mechanisms involved in oxidative stress and inflammatory response caused by low-dose CdTe QDs. The *in vitro* model first demonstrated the effects of low dose CdTe QDs on cell viability and membrane lipid peroxidation. CdTe QDs caused decreased viability and induced damage to the cell membranes of KUP5 cells, including membrane fragmentation and content release, which was similar to the cytotoxic reactions induced by CdTe QDs in other cell lines [24,51,52]. However, it is of note that the concentration range used in this study was much lower than that used in most previous studies [18], and significant LDH release and ROS accumulation could still be observed at the non-cytotoxic concentration of 5 nM. As a member of the macrophage family, KUP5 cells are involved in the phagocytosis and signal presentation of xenobiotics, and may produce significant biological changes at non-cytotoxic concentrations by virtue of their high sensitivity. This finding helps to achieve a more sensitive evaluation of the potential toxicity of low dose CdTe QDs in the future. This finding has not been observed in previous studies. Due to the important phagocytotic activity of KUP5 cells, whether intracellular uptake is involved in the damage caused by the *in vitro* exposure to CdTe QDs should also be considered. Thus, we assessed cell uptake using the same concentration (50 nM) at different exposure times, and the results showed that cadmium content in the cells increased over time. KUP5 cells are macrophages and represent the main mechanism in the endocytosis and exocytosis of xenobiotics [33]. Therefore, in the early stages of exposure to CdTe QDs, KUP5 cells can actively participate in QDs uptake and metabolism, but with prolonged exposure, cells can reduce QDs accumulation through self-protective mechanisms such as exogenous activity [24], which is a plausible mechanism to explain why the content of cadmium in cells did not significantly increase after 12 h and 24 h of treatment. In addition, we also quantified the particulate matter uptake after treatment with different concentrations of CdTe QDs at the same exposure timepoints, and the results showed that the higher the dose, the greater the uptake

by KUP5 cells, which was consistent with the observed changes in intracellular ROS storage volume. Since the accumulation of ROS can induce oxidative stress injury, an excessive stress response can also evolve into an inflammatory response; thus, we further measured the levels of inflammatory cytokines in the cell supernatant. Indeed, the levels of IL-1 β , TNF- α , and IL-6 increased consistently with higher CdTe QDs concentrations. This finding provides further evidence that the uptake of CdTe QDs by macrophages can generate ROS and induce an excessive cellular inflammatory response [36,48].

To verify whether the activation of the key inflammatory NF- κ B pathway and the expression of important inflammation-related protein NLRP3 are involved in the inflammatory response induced by low-dose CdTe QDs exposure, we quantified the related proteins. As a multi-functional transcription factor, NF- κ B is normally present in the cytoplasm after binding to I κ B- α in an inactive form. I κ B- α is an inhibitory protein of NF- κ B, when external stimuli act on cells I κ B- α is degraded, and NF- κ B undergoes nuclear translocation to participate in the regulation of the subsequent inflammatory response [53]. This study found that the NF- κ B pathway was activated in KUP5 cells after a low dose CdTe QDs treatment. In addition, the expression of NLRP3, IL-1 β , and caspase-1 gradually increased while the expression of pro-caspase-1 gradually decreased. Therefore, we speculated whether activation of the NF- κ B pathway mediated the assembly of NLRP3 inflammasomes. There are two steps involved in the activation of the NLRP3 inflammasome [39]. The first step is the activation phase, where the activator induces the expression of NF- κ B and MAPK-dependent NLRP3 inflammasomes [54], including NLRP3 activation and pro-IL-1 β production. The second step is the activation stage. After detecting the activation signal, ASC binds NLRP3 protein to the recruited pro-caspase-1. Activated caspase-1 p10/20 cleaves its target substrate, pro-IL-1 β , to form the mature IL-1 β inflammatory cytokine [55]. In summary, low dose CdTe QDs induces NF- κ B pathway activation and NLRP3 inflammasome expression in KUP5 cells. However, whether this activation is mediated by ROS and whether there is an indirect association between the NF- κ B pathway and NLRP3 expression remains to be further demonstrated.

In order to identify the specific mechanism and role of ROS in the activation of the NF- κ B pathway and in the assembly of NLRP3 induced by low dose CdTe QDs, we used the ROS scavenger NAC in further studies. NF- κ B has been shown to be involved in the inflammatory response, and ROS can act as an inducer for the activation of this pathway [56]. We found that by reducing ROS levels, the levels of inflammatory factors IL-1 β , TNF- α , and IL-6 decreased, indicating that ROS was involved in the inflammatory response. In addition, the expression of NF- κ B decreased after NAC treatment, which provided additional support to the conclusion that the NF- κ B pathway could be activated by ROS, and in turn participate in the inflammatory response. Further analysis found that the expression of NF- κ B and NLRP3 were inhibited after ROS clearance by NAC treatment, and the expression of caspase-1 and IL-1 β were decreased while the expressions of pro-caspase-1 and pro-IL-1 β were increased, indicating that pro-caspase-1 failed to shear into mature caspase-1, and further, pro-IL-1 β could not be converted to IL-1 β , suggesting that ROS could directly activate NF- κ B pathway to promote the expression of downstream pro-IL-1 β [57]. These changes in NLRP3 expression may be directly related to ROS production, but the possibility of indirect regulation of NLRP3 inflammasome assembly through NF- κ B pathway cannot be excluded.

To determine whether there is an association between the assembly of the NLRP3 inflammasome and activation of the NF- κ B pathway, we treated cells with DHMEQ, a nuclear translocation inhibitor of NF- κ B, which induces irreversible inhibition of NF- κ B and is often used to inhibit cancer metastasis [58]. Our results confirmed that DHMEQ inhibited the expression of NF- κ B, and NLRP3 was also inhibited at the same time. The expression of the caspase-1 family components revealed that pro-caspase-1 was increased and caspase-1 was decreased after DHMEQ treatment, indicating that the assembly of the NLRP3

inflammasome was inhibited. In addition, the observed decrease in expression of IL-1 β , a key inflammatory factor, can be explained by two mechanisms. First, NLRP3 inflammasome assembly is blocked after NF- κ B nuclear translocation is inhibited and caspase-1 levels are reduced, more specifically, after IL-1 β invertase activity is reduced. Second, the inhibition of the nuclear translocation of NF- κ B leads to a decrease in downstream pro-IL-1 β [30], both of which may lead to the remission of the inflammatory response after DHMEQ treatment [59]. The above pathway analysis explains that ROS can activate NF- κ B pathway-mediated assembly of NLRP3, thereby inducing the inflammatory outcome of KUP5 cells.

Finally, *in vivo* experiments further confirmed the *in vitro* findings of our study. After ROS clearance, the degree of pathological damage in liver tissue was reduced, the levels of liver metabolic enzymes AST, ALT and ALP returned to normal, and the levels of the antioxidant HO-1 and NRF2 were increased in the mouse model. More importantly, the proportion of activated macrophages in liver tissue was decreased following ROS clearance, and the expression of NF- κ B and NLRP3 in regions of macrophage aggregation region decreased simultaneously. This high overlap between the activated region of macrophages and the expression of inflammatory proteins as well as the synchronous changes observed after ROS clearance convincingly explained the mechanisms involved in liver damage induced after sub-acute exposure of low dose CdTe QD. QDs activates macrophages and induces the accumulation of ROS, which leads to the imbalance of oxidation and anti-oxidation responses. In turn, oxidative damage gradually evolves into inflammatory damage, which eventually leads to structural damage and abnormal function of normal tissues. However, accidental exposure to CdTe QDs during industrial production or in the environment may lead to acute and chronic exposure. Thus, it is necessary to conduct further research on the implications of short- and long-term exposure to low-doses of CdTe QDs in the future.

Although this study fully demonstrates the toxic effects of low-dose CdTe QDs exposure on liver, there are still some limitations in this study that need to be further addressed for the complex organism as a whole. For example, although the exposure method adopted in this study can more directly observe the role of CdTe QDs after transfusion, the actual exposure method of human body should still be fully considered. Whether the hepatic macrophages used in this study can represent the response characteristics of the entire macrophage family and whether non-hepatic macrophages will be damaged after prolonged low-dose exposure remains to be further studied.

5. Conclusions

We provide a comprehensive summary of the exposure risk to low doses of CdTe QDs, which has not been previously explored. Our study provides an explanation of the toxicity and outcomes to KUP5 cells after treatment with low-dose CdTe QDs. In this study, we found that sub-acute exposure to low-dose CdTe QDs can induce the activation of liver macrophages in the body, which leads to subsequent antioxidant imbalance and to the infiltration of inflammatory cytokines in the liver, and the expression of abnormal liver metabolic enzymes and liver tissue damage. Subsequent *in vitro* models further demonstrated that KUP5 cells could be activated following low dose CdTe QDs uptake, resulting in ROS production. ROS-mediated activation of the NF- κ B pathway can further regulate the assembly of distal NLRP3 inflammasomes, and finally, the inflammatory cascade stimulated by inflammatory cytokines IL-1 β , TNF- α , and IL-6 ultimately leads to KUP5 cell damage. This study highlights the importance of low-dose exposure to CdTe QDs and the key effect of ROS in the mechanisms involved in low-dose CdTe QDs-induced liver injury, via activation of the NF- κ B pathway and indirect promotion of NLRP3 expression. Our findings provide a rationale for countermeasures to counteract the exposure risk of low dose CdTe QDs in the future, and can the identified mechanisms may be targeted to control the toxicity of CdTe QDs.

Authors' contributions

Research Design: ZT, PYT, WDM; Data collection: PYT, WDM; Data analysis and interpretation: PYT. Technical Support: MY, CYN, LQ; Draft Manuscript: PYT; Supervising and coordinating research: ZT, TM, PYP; Key revisions and final submission decisions: All authors. The author read and approved the final manuscript.

Declaration of competing interest

None.

Funding

This work was supported by the National Natural Science Foundation of China (No. 81673218), the Natural Science Foundation of Jiangsu Province (No. BK20201268).

Declaration of interests

The authors declare that they have no known competing financial interests or personal relationships that could have appeared to influence the work reported in this paper.

Acknowledgements

The authors wish to express gratitude the Key Laboratory of Environmental Medical Engineering, Ministry of Education, School of Public Health, Southeast University for providing a good experimental environment and advanced equipment and technical support. We thank the Laboratory Animal Management Committee of Southeast University for the careful care and cultivation of the animals needed for the experiment. Thanks to the Animal Experiment Ethics Review Committee of Southeast University for approving this study (Approval Number. 20200405016).

Appendix A. Supplementary data

Supplementary data to this article can be found online at <https://doi.org/10.1016/j.redox.2021.102157>.

References

- [1] F. Shahdost-Fard, N. Fahimi-Kashani, M.R. Hormozi-Nezhad, A ratiometric fluorescence nanosensor using CdTe QDs for fast detection of carbaryl insecticide in apple, *Talanta* 221 (2021) 121467.
- [2] J. Xiao, G. Kai, X. Chen, Effect of CdTe QDs on the protein-drug interactions, *Nanotoxicology* 6 (3) (2012) 304–314.
- [3] P. Chen, Z. Liu, J. Liu, et al., A novel electrochemiluminescence aptasensor based CdTe QDs@NH₂-MIL-88(Fe) for signal amplification, *Electrochim. Acta* 354 (2020) 136644.
- [4] P. Chen, R. Qu, W. Peng, et al., Visual and dual-fluorescence homogeneous sensor for the detection of pyrophosphatase in clinical hyperthyroidism samples based on selective recognition of CdTe QDs and coordination polymerization of Ce³⁺, *J. Mater. Chem. C* 9 (12) (2021) 4141–4149.
- [5] B. Hosnedlova, M. Vsetickova, M. Stankova, et al., Study of physico-chemical changes of CdTe QDs after their exposure to environmental conditions, *Nanomaterials* 10 (5) (2020) 865.
- [6] X. Xiang, T. Gao, B.R. Zhang, et al., Surface functional groups affect CdTe QDs behavior at mitochondrial level, *Toxicology Research* 7 (6) (2018) 1071–1080.
- [7] L. Lai, J. Jin, Z. Xu, et al., Spectroscopic and microscopic studies on the mechanism of mitochondrial toxicity induced by CdTe QDs modified with different ligands, *J. Membr. Biol.* 248 (4) (2015) 727–740.
- [8] R. Landsiedel, A. Oomen, P. Bos, et al., NanoSafetyVision: toxicity testing strategy for nanomaterials, *Toxicol. Lett.* 211 (Supplement) (2012) S179.
- [9] M.T. Hasan, B.H. Lee, C.W. Lin, et al., Near-infrared emitting graphene quantum dots synthesized from reduced graphene oxide for in vitro/in vivo/ex vivo bioimaging applications, *2D Mater.* 8 (3) (2021) 035013.
- [10] A. Keramanizadeh, N.R. Jacobsen, M. Roursgaard, et al., Hepatic hazard assessment of silver nanoparticle exposure in healthy and chronically alcohol fed mice, *Toxicol. Sci.* 158 (1) (2017) 176–187.
- [11] F. Zheng, J. Zhou, Z. Ouyang, et al., Development and characterization of nanobodies targeting the kupffer cell, *Front. Immunol.* 12 (2021) 391.

- [12] Y. Yang, T. Zhao, T. Cheng, et al., Hepatotoxicity induced by ZnO quantum dots in mice, *RSC Adv.* 4 (11) (2014) 5642–5648.
- [13] J. Fan, S. Wang, X. Zhang, et al., Quantum dots elicit hepatotoxicity through lysosome-dependent autophagy activation and reactive oxygen species production, *ACS Biomater. Sci. Eng.* 4 (4) (2018) 1418–1427.
- [14] D. Askri, S. Ouni, S. Galai, et al., Nanoparticles in foods? A multiscale physiopathological investigation of iron oxide nanoparticle effects on rats after an acute oral exposure: trace element biodistribution and cognitive capacities, *Food Chem. Toxicol.* 127 (2019) 173–181.
- [15] X. Zhang, X. Guo, X. Kang, et al., Surface functionalization of pegylated gold nanoparticles with antioxidants suppresses nanoparticle-induced oxidative stress and neurotoxicity, *Chem. Res. Toxicol.* 33 (5) (2020) 1195–1205.
- [16] Y. Zhang, W. Poon, A. Tavares, et al., Nanoparticle-liver interactions: cellular uptake and hepatobiliary elimination, *J. Contr. Release* 240 (2016) 332–348.
- [17] X. Zhang, J. Luan, W. Chen, et al., Mesoporous silica nanoparticles induced hepatotoxicity via NLRP3 inflammasome activation and caspase-1-dependent pyroptosis, *Nanoscale* 10 (19) (2018) 9141–9152.
- [18] D. Wu, J. Lu, Y. Ma, et al., Mitochondrial dynamics and mitophagy involved in MPA-capped CdTe quantum dots-induced toxicity in the human liver carcinoma (HepG2) cell line, *Environ. Pollut.* 274 (2021) 115681.
- [19] Z. Wang, S. Han, X. Chen, et al., Eva1a inhibits NLRP3 activation to reduce liver ischemia-reperfusion injury via inducing autophagy in kupffer cells, *Mol. Immunol.* 132 (2021) 82–92.
- [20] X. Xu, Z. Feng, D. Cao, et al., SCARF1 promotes M2 polarization of Kupffer cells via calcium-dependent PI3K-AKT-STAT3 signalling to improve liver transplantation, *Cell Prolif.* 54 (4) (2021) e13022.
- [21] M.S. Stan, S. Badae, A. Hermenean, et al., New insights into the cell death signaling pathways triggered by long-term exposure to silicon-based quantum dots in human lung fibroblasts, *Nanomaterials* 11 (2) (2021) 323.
- [22] Y. Liang, T. Zhang, M. Tang, Toxicity of quantum dots on target organs and immune system, *J. Appl. Toxicol.* (2021).
- [23] F. Ruan, R. Liu, K. Wang, et al., Cytotoxicity of black phosphorus quantum dots on lung-derived cells and the underlying mechanisms, *J. Hazard Mater.* 402 (2021) 122875.
- [24] X. Liang, T. Wu, Y. Wang, et al., CdTe and CdTe@ZnS quantum dots induce IL-1 β -mediated inflammation and pyroptosis in microglia, *Toxicol. In Vitro* 65 (104827) (2020).
- [25] R. Canaparo, F. Foglietta, T. Limongi, et al., Biomedical applications of reactive oxygen species generation by metal nanoparticles, *Materials* 14 (1) (2021) 53.
- [26] Q. Abbas, B. Yousaf, H. Ullah, et al., Environmental transformation and nanotoxicity of engineered nano-particles (ENPs) in aquatic and terrestrial organisms, *Crit. Rev. Environ. Sci. Technol.* 50 (23) (2020) 2523–2581.
- [27] N. Liu, M. Tang, Toxicity of different types of quantum dots to mammalian cells in vitro: an update review, *J. Hazard Mater.* 399 (2020) 122606.
- [28] V. Vilas-Boas, M. Vinken, Hepatotoxicity induced by nanomaterials: mechanisms and in vitro models, *Arch. Toxicol.* 95 (1) (2021) 27–52.
- [29] J. Lu, M. Tang, T. Zhang, Review of toxicological effect of quantum dots on the liver, *J. Appl. Toxicol.* 39 (1) (2019) 72–86.
- [30] D. Wu, Y. Ma, Y. Cao, et al., Mitochondrial toxicity of nanomaterials, *Sci. Total Environ.* 702 (2020) 134994.
- [31] Y. Wang, M. Tang, Review of in vitro toxicological research of quantum dot and potentially involved mechanisms, *Sci. Total Environ.* 625 (2018) 940–962.
- [32] K. He, X. Liang, T. Wei, et al., A metabolomics study: CdTe/ZnS quantum dots induce polarization in mice microglia, *Chemosphere* 246 (2020) 125629.
- [33] K. He, X. Liang, T. Wei, et al., DNA damage in BV-2 cells: an important supplement to the neurotoxicity of CdTe quantum dots, *J. Appl. Toxicol.* 39 (3) (2019) 525–539.
- [34] L. Kong, T. Zhang, M. Tang, et al., Apoptosis induced by cadmium selenide quantum dots in JB6 cells, *J. Nanosci. Nanotechnol.* 12 (11) (2012) 8258–8265.
- [35] M. Himly, M. Geppert, S. Hofer, et al., When would immunologists consider a nanomaterial to be safe? Recommendations for planning studies on nanosafety, *Small* 16 (21) (2020) e1907483.
- [36] X. Wang, C. Chang, J. Jiang, et al., Mechanistic differences in cell death responses to metal-based engineered nanomaterials in kupffer cells and hepatocytes, *Small* 16 (21) (2020) e200052.
- [37] B. Zheng, M. Guo, X. Song, et al., Reversing the systemic biotoxicity of nanomaterials by downregulating ROS-related signaling pathways in the multi-organs of Zebrafish embryos, *Mater Chem Front.* 5 (11) (2021) 4231–4243.
- [38] M. Zhang, Y. Jiang, Y. Yang, et al., Cigarette smoke extract induces pyroptosis in human bronchial epithelial cells through the ROS/NLRP3/caspase-1 pathway, *Life Sci.* 269 (2021) 119090.
- [39] L. Hou, L. Yang, N. Chang, et al., Macrophage sphingosine 1-phosphate receptor 2 blockade attenuates liver inflammation and fibrogenesis triggered by NLRP3 inflammasome, *Front. Immunol.* 11 (2020) 1149.
- [40] Y. Yao, Y. Zang, J. Qu, et al., The toxicity of metallic nanoparticles on liver: the subcellular damages, mechanisms, and outcomes, *Int. J. Nanomed.* 14 (2019) 8787–8804.
- [41] X. Jia, T. Qiu, X. Yao, et al., Arsenic induces hepatic insulin resistance via mtROS-NLRP3 inflammasome pathway, *J. Hazard Mater.* 399 (2020) 123034.
- [42] A. Kumar, A. Pandey, S. Singh, et al., A flow cytometric method to assess nanoparticle uptake in bacteria, *Cytometry Part A* 79A (9) (2011) 707–712.
- [43] Y. Toduka, T. Toyooka, Y. Ibuki, Flow cytometric evaluation of nanoparticles using side-scattered light and reactive oxygen species-mediated fluorescence-correlation with genotoxicity, *Environ. Sci. Technol.* 46 (14) (2012) 7629–7636.
- [44] K.C. Nguyen, Y. Zhang, J. Todd, et al., Biodistribution and systemic effects in mice following intravenous administration of cadmium telluride quantum dot nanoparticles, *Chem. Res. Toxicol.* 32 (8) (2019) 1491–1503.
- [45] J. Li, X. Wang, C.H. Chang, et al., Nanocellulose length determines the differential cytotoxic effects and inflammatory responses in macrophages and hepatocytes, *Small* 17 (38) (2021) e2102545.
- [46] R.C.R. Meex, E.E. Blaak, Mitochondrial dysfunction is a key pathway that links saturated fat intake to the development and progression of NAFLD, *Mol. Nutr. Food Res.* 65 (1) (2021) e1900942.
- [47] Liu T., Lv Y., Zhao J.L., et al., Regulation of Nrf2 by phosphorylation: consequences for biological function and therapeutic implications, *Free Radic. Bio. Med.* 168 (2021) 129–141.
- [48] C.H. Lin, M.H. Yang, L.W. Chang, et al., Cd/Se/Te-based quantum dot 705 modulated redox homeostasis with hepatotoxicity in mice, *Nanotoxicology* 5 (4) (2011) 650–663.
- [49] K.C. Nguyen, W.G. Willmore, A.F. Tayabali, Cadmium telluride quantum dots cause oxidative stress leading to extrinsic and intrinsic apoptosis in hepatocellular carcinoma HepG2 cells, *Toxicology* 306 (2013) 114–123.
- [50] V. Mirshafiee, B. Sun, C.H. Chang, et al., Toxicological profiling of metal oxide nanoparticles in liver context reveals pyroptosis in kupffer cells and macrophages versus apoptosis in hepatocytes, *ACS Nano* 12 (4) (2018) 3836–3852.
- [51] T. Wu, K. He, Q. Zhan, et al., Partial protection of N-acetylcysteine against MPA-capped CdTe quantum dot-induced neurotoxicity in rat primary cultured hippocampal neurons, *Toxicol. Res.* 4 (6) (2015) 1613–1622.
- [52] T. Zhang, Y. Hu, M. Tang, et al., Liver toxicity of cadmium telluride quantum dots (CdTe QDs) due to oxidative stress in vitro and in vivo, *Int. J. Mol. Sci.* 16 (10) (2015) 23279–23299.
- [53] M.J. Kim, J.G. Kim, K.M. Sydara, et al., Croton hirtus L'her extract prevents inflammation in RAW264.7 macrophages via inhibition of NF-kappa B signaling pathway, *J. Microbiol. Biotechnol.* 30 (4) (2020) 490–496.
- [54] Y. Lu, S. Xu, H. Chen, et al., CdSe/ZnS quantum dots induce hepatocyte pyroptosis and liver inflammation via NLRP3 inflammasome activation, *Biomaterials* 90 (2016) 27–39.
- [55] T. Wu, X. Liang, K. He, et al., The role of NLRP3 inflammasome activation in the neuroinflammatory responses to Ag2Se quantum dots in microglia, *Nanoscale* 11 (43) (2019) 20820–20836.
- [56] R. Canaparo, F. Foglietta, T. Limongi, et al., Biomedical applications of reactive oxygen species generation by metal nanoparticles, *Materials* 14 (1) (2021) 14.
- [57] X. Tao, X. Wan, D. Wu, et al., A tandem activation of NLRP3 inflammasome induced by copper oxide nanoparticles and dissolved copper ion in J774A.1 macrophage, *J. Hazard Mater.* 411 (2021) 125134.
- [58] Y. Lin, T. Ukaji, N. Koide, et al., Inhibition of late and early phases of cancer metastasis by the NF-kappaB inhibitor DHMEQ derived from microbial bioactive metabolite epoxyquinomicin: a review, *Int. J. Mol. Sci.* 19 (3) (2018) 729.
- [59] K.H. Lee, J. Lee, J. Woo, et al., Proteasome inhibitor-induced IkkappaB/NF-kappaB activation is mediated by nrf2-dependent light chain 3B induction in lung cancer cells, *Mol. Cells* 41 (12) (2018) 1008–1015.